Air Gap and Edge Effect in the 2D/1D Method with the Magnetic Vector Potential A using MSFEM

Karl Hollaus[1], Joachim Schöberl[1], and Markus Schöbinger[1]

[1]Technische Universität Wien, Institute for Analysis and Scientific Computing, Vienna, Austria
karl.hollaus@tuwien.ac.at

***Abstract*—Eddy currents are simulated in a single laminate representing the whole core of an electrical machine. Despite this drastic reduction of the complexity of the problem a three-dimensional (3D) finite element method (FEM) turns out to be still too expensive for simulations. To overcome this difficulty two-dimensional/one-dimensional (2D/1D) methods are used. This work presents a solution to take the air gap and the edge effect into account in the 2D/1D method based on the multiscale finite element method (MSFEM) using a magnetic vector potential (MVP) $\boldsymbol{A}$. Linear material properties are assumed and the work is carried out in the frequency domain. The new 2D/1D MSFEM is discussed and various simulation results are presented.**

***Index Terms*—Eddy current problems, edge effect, iron core, lamination, multiscale finite element method MSFEM, magnetic vector potential $\boldsymbol{A}$, 2D/1D method.**

I. Introduction

The accurate simulation of eddy currents in laminated iron cores with the finite element method at minimal computational costs is of great interest in the design of electrical machines. The geometric dimensions are extremely different, compare with Fig. 1. The overall dimensions, the radii R and r and the length L, are in the range of meters, whereas the thickness d of the laminates and the air gaps d_0 in between are fractions of millimeters. Many finite elements are required in an accurate model resulting in extremely large equation systems impossible to solve reasonably. However, a laminated core represents a quasi-periodic structure with period $p = d + d_0$ well suited for the MSFEM.

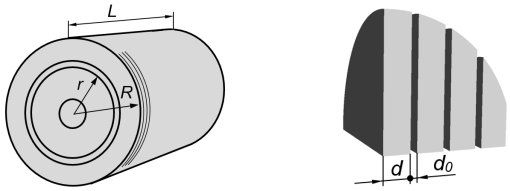

Fig. 1. Large scale: electrical machine with overall dimensions L, R and r, lamination is indicated (left). Fine scale: thickness d of the laminates and the width d_0 of the air gaps (right).

A simple laminate is shown in Fig. 2. In general, there are a magnetic stray field $\boldsymbol{B}_s$ penetrating the plane of the laminate perpendicularly, inducing large eddy current loops $\boldsymbol{J}_s$ on the one hand and on the other the main magnetic field $\boldsymbol{B}_m$, which is parallel to the plane of the laminate and causes eddy currents $\boldsymbol{J}_m$ confined to flow in narrow loops. The eddy currents $\boldsymbol{J}_m$ consist of a laminar part, i.e. currents are flowing parallel to the plane of the laminate, and a part which is perpendicular to the plane, representing the edge effect (EE). It is very common to neglect the end effects, i.e. the stray fields, and therefore, reasonable to assume that all laminates are exposed to the same electromagnetic field distribution. Thus, it suffices to simulate only one single laminate instead of the whole laminated core.

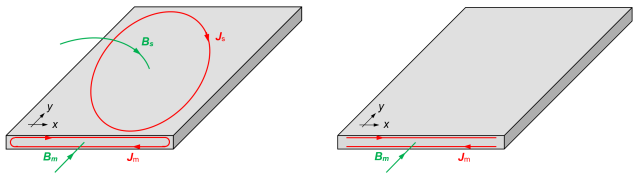

Fig. 2. Magnetic fields and eddy currents in general associated with a laminate (left), without stray field $\boldsymbol{B}_s$ and currents $\boldsymbol{J}_s$ and without edge effect (right).

Brute force 3D finite element (FE) models are still too expensive [1]. To avoid 3D FE models for simulations, the problem is solved using ideas of the MSFEM [2] and 2D/1D methods [3], [4], which are very efficient for this specific purpose. Significant shortcomings of the methods based on the MVP $\boldsymbol{A}$ are the inability to consider an air gap and the EE, [5], [6]. The 2D/1D method with a current vector potential $\boldsymbol{T}$ considers an air gap and the EE almost for free [7].
For example, the EE is relevant in simulations of narrow ferromagnetic strips [8] and for material degradation due to punching etc., [9]. The inclusion of the air gap can easily be substantiated. The overall dimensions of electrical machines include the air gaps. Assuming iron only would improperly lead to essentially higher losses for the same magnetic flux.
The new 2D/1D method with a MVP copes with both the EE and an air gap and performs excellently. Therefore, it is an attractive alternative to brute force 3D FEMs.

II. The Multiscale Finite Element Method

A suitable selection of the local basis is essential for a well performing MSFEM [10]. Only odd polynomials are relevant using a MVP. Gauss-Lobatto polynomials

$$\phi_1(s) = s, \quad \phi_3(s) = \frac{1}{2}\sqrt{\frac{5}{2}}(s^2-1)s, \\ \phi_5(s) = \frac{1}{8}\sqrt{\frac{9}{2}}(s^2-1)(7s^2-3)s, \ldots \tag{1}$$

are used as micro-shape functions (MSFs) ϕ_i with the mapping $s = 2z/d$, where $s \in [-1,1]$ and $z \in [-d/2, d/2]$. Figure 3 shows how the MSFs fit into the periodic structure with p. They are extended by zero in $[-(d+d_0)/2, -d/2]$ and $[d/2, (d+d_0)/2]$ including the air gap, except ϕ_1^0 and ϕ_1, which are extended linearly and become ± 1 and 0 in $\{-(d+d_0)/2, (d+d_0)/2\}$, respectively. These polynomials facilitate the required continuity of the unknown solution and ϕ_1^0 allows to prescribe essential boundary conditions.

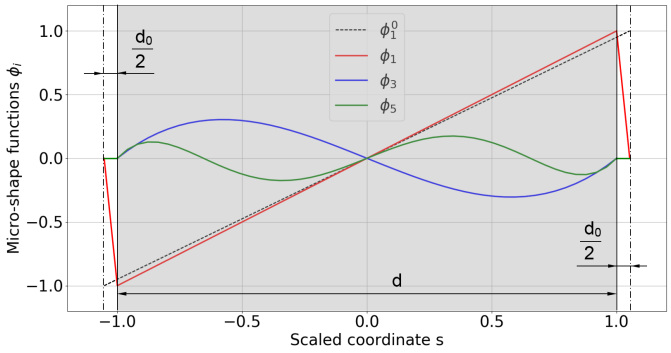

Fig. 3. Micro-shape functions, the grey interval $[-1, 1]$ represents the iron laminate and beyond that up to the dash-dotted line there is the air gap.

III. The 2D/1D Method with $\boldsymbol{A}$ Using MSFEM

The idea is to write the 2D/1D MSFEM approach $\tilde{\boldsymbol{u}}$ as a truncated sum

$$\tilde{\boldsymbol{u}}(x, y, z) \approx \sum_i L_i \phi_i(z) \boldsymbol{u}_i(x, y) \tag{2}$$

based on the space splitting $\Omega = \Omega_{2D} \times [-\frac{d+d_0}{2}, \frac{d+d_0}{2}]$, where L_i is a linear differential operator, either the gradient or the identity operator, and the unknown functions $\boldsymbol{u}_i(x, y)$. The tilde marks the multiscale approach. The approach (2) has two advantages compared to 3D-FEMs, the unknown functions $\boldsymbol{u}_i$ depend solely on x and y and it assumes only odd polynomials in z.

A. Old 2D/1D MSFEM approach

The original approach

$$\tilde{\boldsymbol{A}} = \phi_1(z)\,\mathrm{grad}(u_1(x, y)) + \phi_3(z)\boldsymbol{A}_3(x, y) + \phi_5(z)\boldsymbol{A}_5(x, y) + \ldots \tag{3}$$

with $u_{1h} \in H^1(\Omega_{2D})$ and $\boldsymbol{A}_{3h}, \boldsymbol{A}_{5h}, \ldots \in H(\mathrm{curl}, \Omega_{2D})$ considered neither an air gap nor the EE, see Fig. 4. Here, the third and fifth order term in (3) represent the higher order approach and ϕ_1 is restricted to iron.

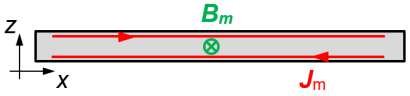

Fig. 4. A single laminate with eddy currents without EE, main magnetic field B_m and associated currents J_m.

B. New 2D/1D MSFEM approach

The new 2D/1D MSFEM approach

$$\tilde{\boldsymbol{A}} = \phi_1^0(z)\,\mathrm{grad}(u_1(x, y)) + \phi_1(z)\boldsymbol{A}_1(x, y) + \mathrm{grad}(w_1(x, y)\phi_1(z)) \tag{4}$$

with $\boldsymbol{A}_{1h} \in H(\mathrm{curl}, \Omega_{2D})$ and $u_{1h}, w_{1h} \in H^1(\Omega_{2D})$ uses two different linear MSFs, ϕ_1 and ϕ_1^0 are shown in Fig. 3. The support for both functions is iron and air. The first term in (4) prescribes an average magnetic flux density or a total magnetic flux, the second term splits the total flux into a major

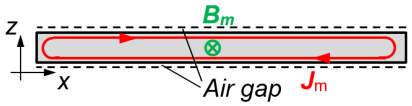

Fig. 5. A single laminate with eddy currents with EE and air gap, main magnetic field B_m and associated currents J_m.

and a minor part flowing through the iron and the air gap, respectively, and corrects the laminar currents according to the corrected flux in iron. The third term considers the EE. Only through the selection of both linear MSFs, ϕ_1^0 and ϕ_1, the introduction of the third term has become feasible.

1) Excitation, boundary conditions: A total magnetic flux Φ through the cross section S in Fig. 6 can be prescribed by

$$\Phi = \int_S \boldsymbol{B}_m \cdot \boldsymbol{e}_y \, dS = \int_S \mathrm{curl}\, \tilde{\boldsymbol{A}} \cdot \boldsymbol{e}_y \, dS = \int_S \mathrm{curl} \left(\phi_1^0(z)\,\mathrm{grad}(u_1(x, y)) + \phi_1(z)\boldsymbol{A}_1(x, y) \right) \cdot \boldsymbol{e}_y \, dS = \int_{-\frac{d+d_0}{2}}^{\frac{d+d_0}{2}} \phi_{1,z}^0 \, dz \int_0^w u_{1,x} \, dx = 2(u_1(w, y) - u_1(0, y)) = 2C \tag{5}$$

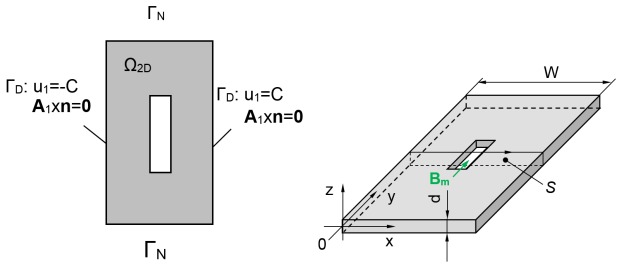

Fig. 6. Boundary conditions for u_1 and $\boldsymbol{A}_1$ representing a flux tube.

2) Weak form of the 2D/1D MSFEM: An eddy current problem in the frequency domain has to be solved using the phasor convention $e^{j\omega t}$. To obtain the weak form of the new 2D/1D MSFEM the approach (4) represents the trial function and according to the Galerkin method the test function

$$\tilde{\boldsymbol{v}} = \phi_1^0(z)\,\mathrm{grad}(v_1(x, y)) + \phi_1(z)\boldsymbol{v}_1(x, y) + \mathrm{grad}(q_1(x, y)\phi_1(z)) \tag{6}$$

is selected. The weak form reads as:
Find $(u_{1h}, \boldsymbol{A}_{1h}, w_{1h}) \in V_D := \{(u_{1h}, \boldsymbol{A}_{1h}, w_{1h}) : u_{1h} \in \mathcal{U}_h, \boldsymbol{A}_{1h} \in \mathcal{V}_h, w_{1h} \in \mathcal{W}_h, u_{1h} = u_D$ and $\boldsymbol{A}_{1h} \times \boldsymbol{n} = \boldsymbol{0}$ on $\Gamma_D\}$, such that

$$\int_\Omega \mu^{-1}\,\mathrm{curl}(\tilde{\boldsymbol{A}}) \cdot \mathrm{curl}(\tilde{\boldsymbol{v}})\, d\Omega + j\omega \int_\Omega \sigma \tilde{\boldsymbol{A}} \cdot \tilde{\boldsymbol{v}}\, d\Omega = 0 \tag{7}$$

for all $(v_{1h}, \boldsymbol{v}_{1h}, q_{1h}) \in V_0$.
We propose to use the finite element subspaces $\mathcal{U}_h \subset H^1(\Omega_{2D})$, $\mathcal{V}_h \subset H(\mathrm{curl}, \Omega_{2D})$ and $\mathcal{W}_h \subset H^1(\Omega_{2D})$, respectively. The micro-shape functions ϕ_i are in the space of continuous and periodic functions $H_{per}(\Omega)$.
Essential boundary conditions are prescribed on $\Gamma_D \subset \partial\Omega_{2D}$. Since the problem is linear and due to the space splitting approach the integrations in (7) over $[-(d+d_0)/2, (d+d_0)/2]$ can be carried out analytically.

IV. Numerical example

The laminate in Fig. 7 with a hole arranged symmetrically in the center has been chosen to study in particular the EE. The material parameters $\sigma = 2.08 \cdot 10^6 S/m$ and $\mu = 1,000\mu_0$ have been selected. Boundary conditions are prescribed such that a total flux Φ flows from the front $y = 0$ to the back $y = 30mm$ and vice versa according to the time variation. Results obtained by the 2D/1D methods are compared with reference solutions computed with the FEM in 3D using the mixed formulation $\boldsymbol{A}, V-\boldsymbol{A}$ to prescribe the suitable boundary conditions.

A. Results

The number of unknowns and the eddy current losses obtained by the different methods are summarized in Tab. I. Old and New stands for the methods in Secs. III-A and III-B, respectively. Wrong means simply adding the third term in (4) to the lowest order of (3) what seams to be obvious [2]. The computational costs are reduced by the 2D/1D method compared to the FEM 3D enormously.

Table I
Eddy Current Losses

FE model	NDOF H^1 of 3^{rd} order	NDOF $H(curl)$ of 2^{nd} order	Losses μW
FEM 3D		305,203	709
Old	4,675	9,210	718
New	9,350	9,210	712
Wrong	9,350		$115 \cdot 10^3$

Simulations with and without the EE, i.e. considering or neglecting the third term in (4), are present below.

1) Edge effect: Figure 7 show the EE by means of the z-component of the current density $\boldsymbol{J}$. For a fair comparison the scaling of the colors is such that corresponding figures use the same maximum and minimum. The ability to reproduce the EE by the 2D/1D MSFEM with EE is very good. A

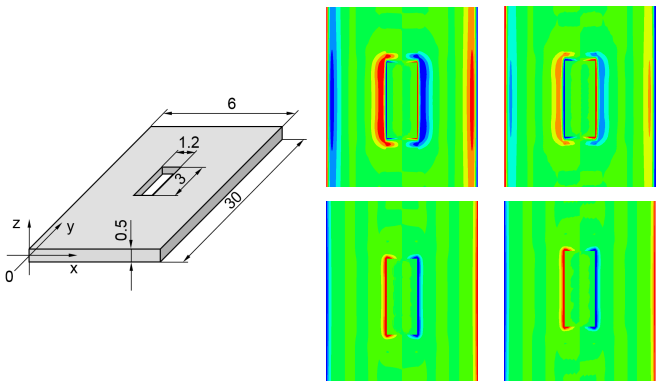

Fig. 7. Laminate with a hole, dimensions in mm (left). Current densities in the vicinity of the hole in the plane of symmetry at $z = 0.0$, 3D SFEM (middle) and the 2D/1D MSFEM with EE (right): z-components $Re\{\boldsymbol{J}_z\}$ (above) and $Im\{\boldsymbol{J}_z\}$ (below), $f = 1,000Hz$.

comparison of the x-component of the current densities with and without EE is shown in Fig. 8. It is easy to see, that the method without EE completely fails. A large difference is apparent. However, the method with EE copes with the EE very well.

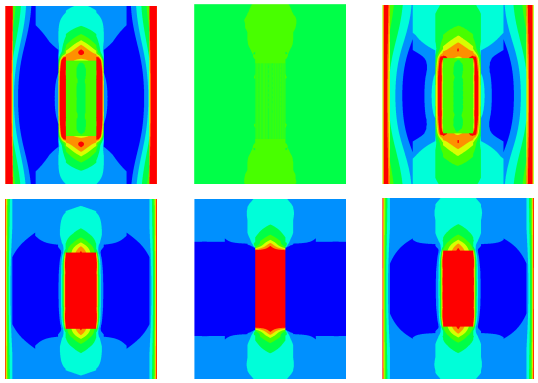

Fig. 8. Current densities in the vicinity of the hole in the plane at $z = 1.8mm$, 3D SFEM (left), the 2D/1D MSFEM without EE (middle) and the 2D/1D MSFEM with EE (right): x-components $Re\{\boldsymbol{J}_x\}$ (above) and $Im\{\boldsymbol{J}_x\}$ (below), $f = 1,000Hz$.

2) Planes of symmetry: Apart from $z = 0$, which exists always for this kind of 2D/1D problems, there are two planes of symmetry, see Fig. 9. Making use of the symmetry, only one quarter has to be simulated. Red boundary conditions are new or modified compared to the entire problem. Exploiting the symmetry works very well as shown in Fig. 9. Simulations have shown, that the first three or four significant digits of the eddy current losses agree.

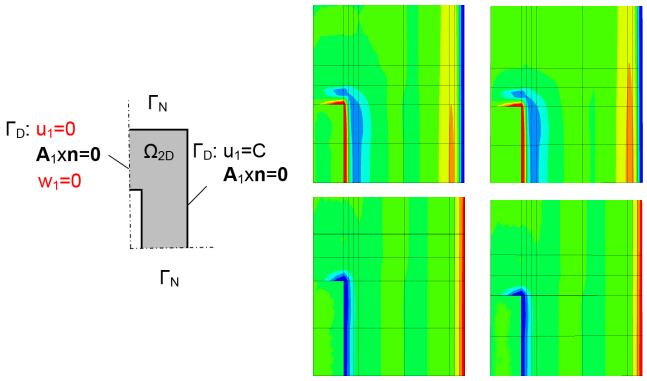

Fig. 9. Boundary conditions for u_1, $\boldsymbol{A}_1$ and w_1, $\Gamma_D \cup \Gamma_N = \partial\Omega_{2D}$, hole is included in Ω_{2D} (left). Current densities in the vicinity of the hole in the plane of symmetry at $z = 0.0$, 2/1D MSFEM with EE, entire problem (middle) and one quarter (right): z-components $Re\{\boldsymbol{J}_z\}$ (above) and $Im\{\boldsymbol{J}_z\}$ (below), $f = 1,000Hz$.

V. Higher order 2D/1D MSFEM

Frequency sweeps of the losses have been simulated too.

A. Linear 2D/1D MSFEM

There is a clear difference between the methods with and without EE as can be seen easily in Fig. 10. Both methods allow only a liner approximation. That's why the error starts to grow already at low frequencies.

B. Higher order 2D/1D MSFEM approach

To overcome this severe limitation higher order terms, third order and fifth order and so on, are added to the linear approach (4) leading the higher order 2D/1D MSFEM

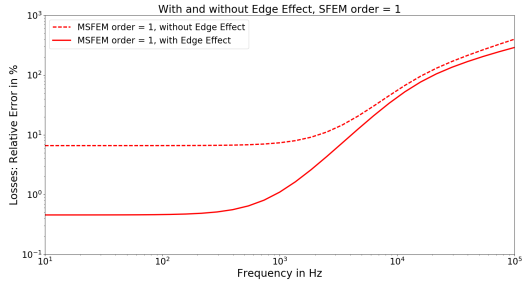

Fig. 10. The relative error of the eddy current losses versus frequency of the linear 2D/1D MSFEMs.

$$\begin{aligned} \tilde{\boldsymbol{A}} = \phi_1^0(z)\,\mathrm{grad}(u_1(x,y)) \;+\; \\ \phi_1(z)\boldsymbol{A}_1(x,y) + \mathrm{grad}(w_1(x,y)\phi_1(z)) \;+\; \\ \phi_3(z)\boldsymbol{A}_3(x,y) + \mathrm{grad}(w_3(x,y)\phi_3(z)) \;+\; \\ \phi_5(z)\boldsymbol{A}_5(x,y) + \mathrm{grad}(w_5(x,y)\phi_5(z)) \;+\; \ldots \end{aligned} \tag{8}$$

The associated test function is constructed and the weak form is derived analogue to the first order 2D/1D MSFEM (6) and (7), respectively. Higher order methods perform clearly better than the linear methods at higher frequencies as demonstrated in Figs. 11 and 12. The higher the order the better the methods perform. Considering the EE provides essentially more accurate losses in a wide frequency range. The peak

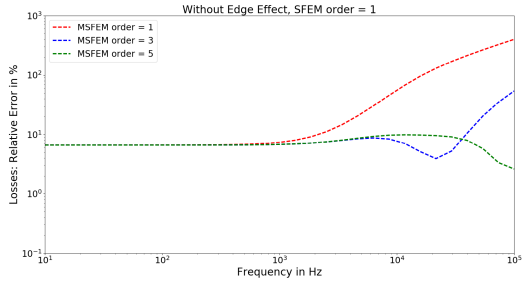

Fig. 11. The relative error of the eddy current losses versus frequency of higher order 2D/1D MSFEMs without EE.

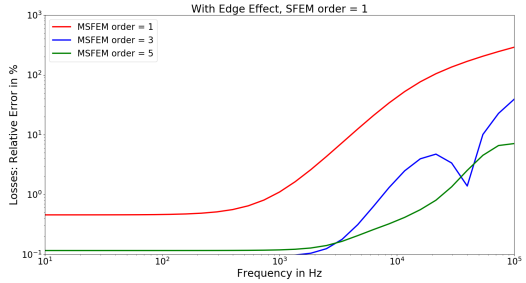

Fig. 12. The relative error of the eddy current losses versus frequency of higher order 2D/1D MSFEMs with EE.

in the third order method can easily be explained by the fact, that the relative errors change their sign versus frequency. This becomes visible using a linear scale for the error. For example, the third order 2D/1D MSFEM changes the sign at about 30,000Hz as shown in Fig. 13.

C. Computational costs

The number of degrees of freedom (DOFs) are much smaller than that of 3D SFEM. Note, that also the coupling of the

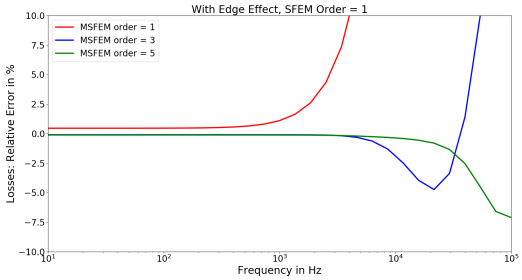

Fig. 13. The relative error of the eddy current losses versus frequency of higher order 2D/1D MSFEMs with EE, linear scale of the error, detail.

unknowns in 3D SFEM is much stronger. The 3D SFEM uses a mesh which is relatively fine to evaluate the relative errors in Secs. V and VI. accurately. The number of DOFs can be reduced by the 2D/1D MSFEM essentially.

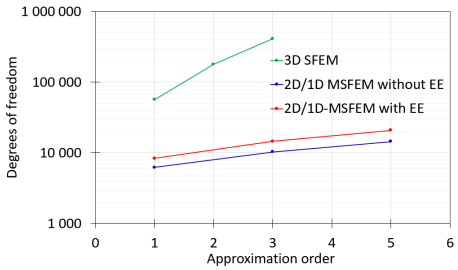

Fig. 14. Computational costs in terms of unknowns.

Acknowledgment

This work was supported by the Austrian Science Fund (FWF) under projects P 27028 and P 31926.

References

[1] P. Handgruber, A. Stermecki, O. Bíró, A. Belahcen, and E. Dlala, "Three-Dimensional Eddy-Current Analysis in Steel Laminations of Electrical Machines as a Contribution for Improved Iron Loss Modeling," *IEEE Trans. Ind. Appl.*, vol. 49, no. 5, pp. 2044–2052, Sept 2013.

[2] K. Hollaus and J. Schöberl, "Some 2-D Multiscale Finite-Element Formulations for the Eddy Current Problem in Iron Laminates," *IEEE Transactions on Magnetics*, vol. 54, no. 4, pp. 1–16, April 2018.

[3] O. Bottauscio, M. Chiampi, and D. Chiarabaglio, "Advanced model of laminated magnetic cores for two-dimensional field analysis," *IEEE Trans. Magn.*, vol. 36, no. 3, pp. 561–573, 2000.

[4] J. Pippuri, A. Belahcen, E. Dlala, and A. Arkkio, "Inclusion of Eddy Currents in Laminations in Two-Dimensional Finite Element Analysis," *IEEE Trans. Magn.*, vol. 46, no. 8, pp. 2915–2918, 2010.

[5] O. Bottauscio and M. Chiampi, "Analysis of laminated cores through a directly coupled 2-D/1-D electromagnetic field formulation," *IEEE Trans. Magn.*, vol. 38, no. 5, pp. 2358–2360, 2002.

[6] P. Rasilo *et al.*, "Model of laminated ferromagnetic cores for loss prediction in electrical machines," *IET Electr. Power Appl.*, vol. 5, no. 7, pp. 580–588, 2011.

[7] M. Schöbinger, J. Schöberl, and K. Hollaus, "MSFEM for the Linear 2D/1D-Problem of Eddy Currents in Thin Iron Sheets," *IEEE Trans. Magn., accepted Oct. 2018, 10 pages.*, April 2018.

[8] O. Bottauscio, M. Chiampi, and D. Chiarabaglio, "Magnetic flux distribution and losses in narrow ferromagnetic strips," *J. Magn. Magn. Mater.*, vol. 215 - 216, pp. 46 – 48, 2000.

[9] M. Bali, H. D. Gersem, and A. Muetze, "Finite-Element Modeling of Magnetic Material Degradation Due to Punching," *IEEE Trans. Magn.*, vol. 50, no. 2, pp. 745–748, Feb 2014.

[10] I. Babuska and J. M. Melenk, "THE PARTITION OF UNITY METHOD," *Int. J. Numer. Meth. Engng.*, vol. 40, pp. 727–758, 1997.